

Electrochemical characterization of Prussian blue type nickel hexacyanoferrate redox mediator for potential application as charge relay in dye-sensitized solar cells

Iwona A. Rutkowska · Adam Andrearczyk ·
Sylvia Zoladek · Monika Goral ·
Kazimierz Darowicki · Pawel J. Kulesza

Received: 4 May 2011 / Revised: 13 July 2011 / Accepted: 14 July 2011 / Published online: 9 August 2011
© The Author(s) 2011. This article is published with open access at Springerlink.com

Abstract A polynuclear electronically/ionically (redox) conducting mixed-valent inorganic material such as nickel (II) hexacyanoferrate(II,III), NiHCF, was considered for potential application as a redox mediator (charge relay) in dye-sensitized solar cell (DSSC). The NiHCF redox reactions were found fast and reversible not only when the system was studied as thin film exposed to an aqueous supporting electrolyte but also as bulk material (pasted powder) in solid state, i.e., in the absence of contact with external liquid electrolyte phase. Usefulness of NiHCF material was diagnosed using conventional electroanalytical approaches, solid-state voltammetric methodology, as well as the dynamic electrochemical impedance spectroscopy technique that permitted monitoring of impedance spectra under potentiodynamic conditions. The material was utilized in a mixed-valent state, i.e., as a mixture of $K_4Ni^{II}[Fe^{II}(CN)_6]$ and $K_3Ni^{II}[Fe^{III}(CN)_6]$ in which iron(II) and iron(III) sites were at the 1:1 ratio. Under such conditions, dynamics of electron-hopping between mixed-valent iron sites was maximized. Our DSSC utilized cis-dithiocyanatobis(4,4'-dicarboxylic acid-2,2'-bipyridine) ruthenium(II) dye (N3) adsorbed onto TiO_2 semiconductor and NiHCF as redox mediator. Although performance of

our DSSC was not optimized in terms of the NiHCF film thickness and morphology, as well as lower photocurrents in comparison to those characteristic of the iodine/iodide based DSSC were obtained, our system yielded readily fairly high open-circuit photovoltages on the level of 800 mV. An important issue was that the formal potential of NiHCF was more positive relative to the potential of the iodide/triiodide couple while being still more negative than that equivalent to the ground state of the N3 dye. Thus, NiHCF mediator was able to regenerate the dye.

Keywords Metal hexacyanoferrate · Sol-gel processed deposits · Solid-state voltammetry charge propagation · Charge relay · Solar cell

Introduction

Recent progress in the area of dye-sensitized solar cells (DSSCs), aiming at the enhancement of their performance, has concerned improvement of morphology of semiconducting materials, optimization of dyes, and the search for novel electrolytes and charge relays (mediators) [1–7]. Successful application of mesoporous TiO_2 (anatase) films in DSSCs [1, 8, 9] was prompted by the systems' nanocrystallinity, highly porous character, and the ability to provide large surface area to adsorb sizeable amounts of dye. The nanostructured morphology of anatase semiconducting particles facilitated interfacial electron transfers to and from dye molecules, close contact, and easy access of the electrolyte ions and charge relay species, thus leading to the appearance of fairly high photovoltages [10, 11]. Nonporous TiO_2 film texture was also of importance when it comes to anchoring photosensitizer (dye) at quasi-monolayer level to ensure efficient light

I. A. Rutkowska · S. Zoladek · M. Goral · P. J. Kulesza (✉)
Department of Chemistry, University of Warsaw,
Pasteura 1,
02-093 Warsaw, Poland
e-mail: pkulesza@chem.uw.edu.pl

A. Andrearczyk · K. Darowicki
Department of Electrochemistry Corrosion and Materials
Engineering, Gdansk University of Technology,
Narutowicza 11/12,
80-233 Gdansk, Poland

harvesting and electron injections. Typical examples of dyes include organometallic compounds in which inorganic element exhibits redox properties in addition to its light sensitivity. The so-called N3 dye, i.e., cis-dithiocyanatoabis (4,4'-dicarboxylic acid-2,2'-bipyridine) ruthenium(II), that is utilized in the present study, can be viewed as a representative example of the robust efficient photosensitizing system.

Charge relay and electrolyte are used not only to permit redox conductivity or appropriate charge propagation between two opposing electrodes but also to ascertain regeneration of a dye. An effective system would be a fast electron-transfer redox mediator (preferably in solid state) characterized by a formal potential fairly close to (but still more negative than) the potential equivalent to energy level of the ground state of the dye used. Although many redox charge relays have been proposed as alternatives to the Γ/I_3^- redox couple and successfully applied in DSSCs [12–15], the semisolid iodine/iodide-based system (dispersed in the appropriate electrolyte-containing solvent mixture) is so far most commonly used and viewed as the most stable and efficient material. Electrolytes based on volatile organic solvents are rather impractical due to their instability during operation at higher temperatures. Recently, some efforts have been made to replace the organic solvent electrolytes with p-type inorganic semiconductors [16, 17], polymer electrolytes [18, 19], and organic hole-transport materials [20], but their efficiencies still require improvement. Ionic liquid-based electrolytes have been found promising for DSSCs because of their reasonable conductivity and such features as negligible vapor pressure and non-flammability [21].

In the present work, we consider the ionically (K^+) and electronically (mixed-valence electron-hopping) conducting polynuclear inorganic material, namely Prussian Blue type nickel hexacyanoferrate [22–27] as material for potential application in DSSC as solid redox mediator (charge relay). Redox reactions of metal hexacyanoferrates are fast and reversible, and the systems are characterized by very good chemical and mechanical stability. Here, we have chosen nickel(II) hexacyanoferrate(III,II), NiHCF, as a model cyanometallate material [28–30] because it shows well-defined and reproducible responses not only when studied as thin films exposed to aqueous supporting electrolytes but also in solid state, i.e., in the absence of contact with external liquid phase [29–32]. In addition to these important dynamic features, utilization of NiHCF in DSSC is also justified in thermodynamic terms because the system's formal potential is more positive in comparison to that of the I_3^-/I^- couple (while being still more negative relative to the potential characteristic of the N3 dye's ground energetic state). In this study, we have diagnosed usefulness of NiHCF using conventional electroanalytical approaches, solid-state voltammetric methodology, as well as dynamic

electrochemical impedance spectroscopy (DEIS) technique [33–35] that permits monitoring of impedance spectra under potentiodynamic conditions.

Experimental

Chemicals, materials, and procedures

All chemicals were analytical grade materials and were used as received. Solutions were prepared from the distilled and subsequently deionized water.

Conventional thin films of nickel hexacyanoferrate on glassy carbon electrode were fabricated by electrodeposition through potential cycling (from 0.85 to 0 V for 10 min at 50 mV s^{-1}) in the solution (50 cm^3) formed by mixing 49 cm^3 1.0 mol dm^{-3} KCl with 0.5 cm^3 0.1 mol dm^{-3} $K_3Fe(CN)_6$, 0.5 cm^3 0.1 mol dm^{-3} $NiCl_2$.

The oxidized or reduced form (bulk material) of nickel hexacyanoferrate, NiHCF, was prepared by precipitation (via dropwise mixing) of equivalent amounts of 0.01 mol dm^{-3} solutions: $K_3Fe(CN)_6$, or $K_4Fe(CN)_6$, with 0.01 mol dm^{-3} $NiSO_4$ (containing 0.01 mol dm^{-3} EDTA and 0.5 mol dm^{-3} K_2SO_4 adjusted to pH=4 with diluted H_2SO_4). The procedure was analogous to that described earlier except that it involved addition of EDTA. It is noteworthy that EDTA forms complexes with Ni^{2+} ions, and its presence in the solution results in slower precipitation of NiHCF as well as in the formation of more compact system's granules typically on sub-micrometer (down to tens of nanometer) level. As a rule, suspensions of both oxidized and reduced NiHCF forms were left overnight to complete precipitation. They were subsequently mixed (under magnetic stirring) to produce NiHCF suspension containing mixed-valence $-Fe^{III,II}(CN)_6$ sites at approximately 1:1 ratio. The resulting precipitate was filtered, rinsed carefully with water, and air-dried for 24 h before grinding with pestle and mortar. The degree of hydration (approximately 10–15 stoichiometric water molecules per

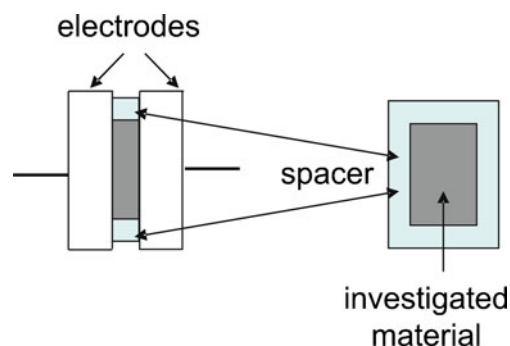


Fig. 1 Two-electrode design for solid-state voltammetric measurements performed in the absence of liquid electrolyte phase

NiHCF unit) was estimated from the hydrogen content (elemental analysis).

Mesoporous TiO_2 films (thickness, approximately $2.5 \mu\text{m}$) were prepared from commercial Degussa P25 TiO_2 powder (average diameter of particles, 25 nm) composed of approximately 80% anatase and 20% rutile. They were deposited on conducting F-doped SnO_2 -coated glass (sheet resistance, 10Ω per square) by spray pyrolysis as described elsewhere [36]. Mesoporous TiO_2 layers were pressed onto the spray layer using the approach described before [37]. Here 2 g of TiO_2 powder (Degussa P25, average diameter 25 nm) was suspended in 10 ml of pure ethanol by stirring for several hours, followed by sonication for 5 min using the titanium horn immersed in the suspension. The slurry was spread onto the surface of the $\text{SnO}_2/\text{TiO}_2$ substrate by tape-casting, i.e., by using one or more layers of scotch tape ($50 \mu\text{m}$) as spacers. The resulting layer of ethanol/ TiO_2 was allowed to dry in the ambient atmosphere. The TiO_2 layers were then heated for 2 h at 500°C in air. Films were removed from the oven at $\sim 100^\circ\text{C}$ and placed in ethanolic solutions of the dye “N3”, which is $\text{RuL}_2(\text{SCN})_2$ where $L=4,4'$ -dicarboxy-2,2'-bipyridine. The dye was purchased from Solaronix under the name Ruthenium 535. After being dyed overnight, the films were rinsed in ethanol and dried in a stream of compressed air. Before experiments, the photoelectrode was conditioned for 30 min in the freshly prepared solution obtained by mixing of equimolar amounts of $1 \text{ mmol dm}^{-3} \text{ Ni}^{2+}$ and $1 \text{ mmol dm}^{-3} \text{ Fe}(\text{CN})_6^{3-}$ solutions. Slow precipitation of nickel hexacyanoferrate (by sol-gel aggregation) permitted its deposition in the titanium oxide pores.

The nickel hexacyanoferrate-modified dye-adsorbed TiO_2 electrode and counter electrode (platinized F-doped SnO_2 -coated glass) were assembled into a sealed sandwich-type cell in which pasted NiHCNFe powder was introduced between electrodes and the spacing between them (approximately 0.6 mm) was controlled by introducing an appropriate spacer cutout from cardboard paper. The active area of DSSC was fixed to 0.3 cm^2 .

Diagnostic electrochemical measurements

The cell for solid-state (namely in the absence of an external phase of supporting electrolyte) voltammetric experiments utilized two inert glassy carbon slide electrodes (Fig. 1) mounted in a sandwich configuration [30–32] of the 0.3 cm^2 geometric area. The spacing between electrodes (approximately 0.6 mm) was controlled by introducing a spacer cutout from cardboard paper.

The cyanometallate material of mixed-valent NiHCF was introduced (pasted) onto each sandwich-forming glassy carbon electrode. When using a three-electrode potentiostat, the operation of a cell in two-electrode mode implied that

one of these two electrodes was connected as a working electrode and the second one acted as reference and counter electrodes simultaneously [30, 31]. To assure good contact of electrodes with the material, a pressing weight was used. The assembly was enclosed in Teflon tubing and sealed to protect the material from dehydration.

DEIS measurements were performed in a manner described earlier [33–35]. AC perturbation signal was a package of 20, selected sinusoids of different amplitudes, generated by a DXI 6120 National Instruments measurement card. The perturbation signal and additional DC component generated by an Agilent 33120 generator were sent to a KGLstst 4.1 potentiostat. Current–voltage response and the additional voltage signal were registered with PXI-1031DC National Instruments measurement card. The measurement setup was controlled with the LabVIEW software (National Instruments).

Conventional electrochemical measurements were done in a three-electrode mode using CH Instruments (Austin, TX, USA) model 660 analyzer. All potentials were expressed versus the KCl saturated Ag/AgCl reference.

Photoelectrochemical measurements

The photoaction spectra were determined using a 500-W xenon lamp (Ushio UXL-502HSO) set in an Oriel Model 66021 housing and a Multispec 257 monochromator (Oriel) with a bandwidth of 4 nm .

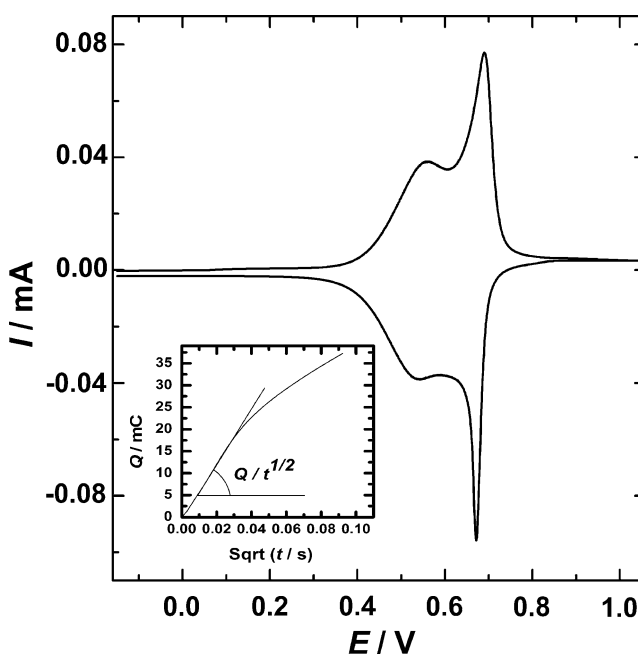


Fig. 2 Cyclic voltammetric response of NiHCF film on glassy carbon electrode recorded in $0.5 \text{ mol dm}^{-3} \text{ K}_2\text{SO}_4$. Scan rate, 50 mV s^{-1} . Inset illustrates chronocoulometric response obtained upon application of the anodic potential step from 0 to 0.85 V

Results and discussion

Diagnostic electrochemical measurements

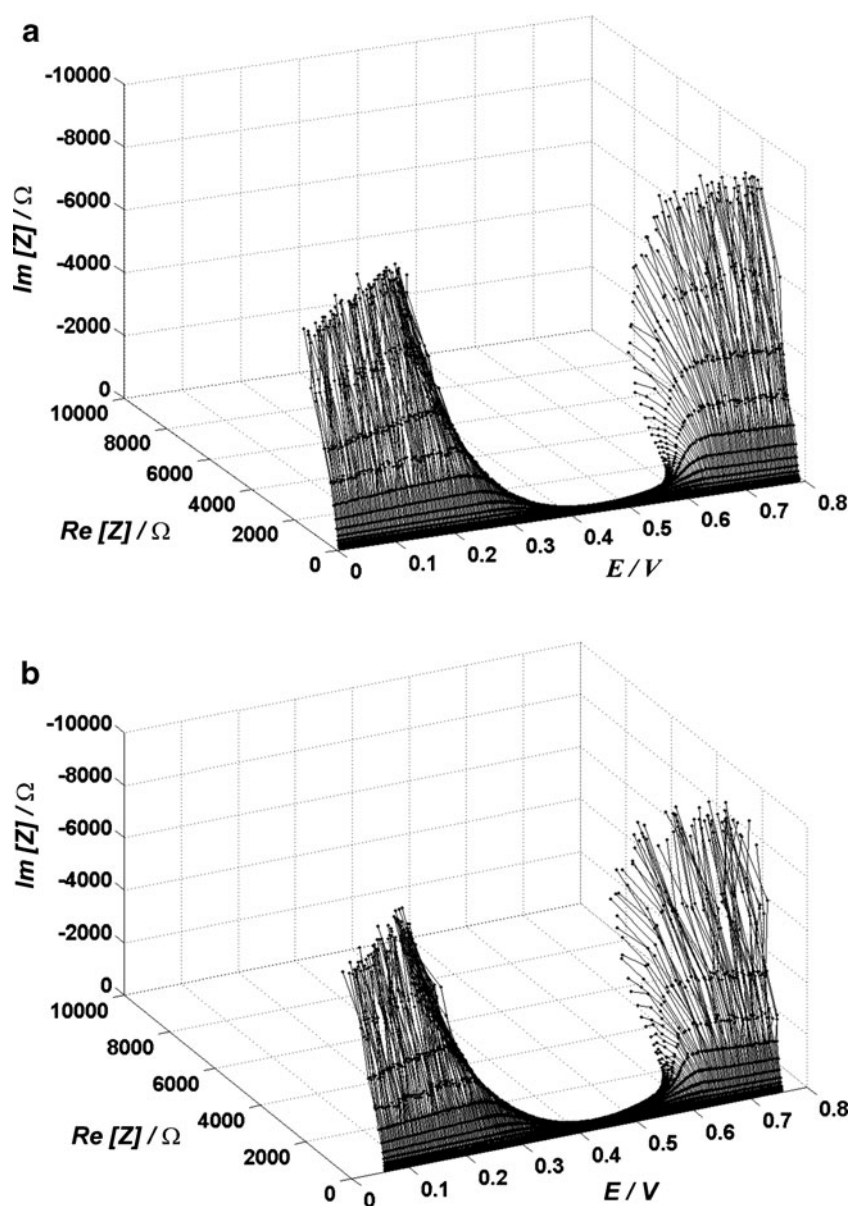
The response of a conventional nickel(II) hexacyanoferrate (II,III) (NiHCF) film on glassy carbon (Fig. 2) is characterized by overlapping redox reactions at about 0.4–0.6 V. Although the approximate formulas $\text{KNi}_{1.5}[\text{Fe}^{\text{II}}(\text{CN})_6]$ and $\text{K}_2\text{Ni}[\text{Fe}^{\text{II}}(\text{CN})_6]$ are usually assigned to two predominant forms of the reduced NiHCF films, in reality the films are electrodeposited (in the presence of K^+ ions) in the form of solid solutions rather than homogeneous phases. The most important observation coming from the above experiments with thin film of nickel(II) hexacyanoferrate(II,III) (exposed to liquid K^+ -containing electrolyte) is the fact that

NiHCF redox transitions, as well as the ability to act as redox mediator, appear at fairly positive potentials (approximately 0.4–0.6 V vs. Ag/AgCl).

In order to be more quantitative about dynamics of charge transport during redox reactions in the NiHCF film described above, we have recorded dependencies (inset of Fig. 2) of the chronocoulometric charge (Q) on the square root of time ($t^{1/2}$) [30, 31] upon application of the potential step from 0 to 0.85 V. The appearance of linear portion in the chronocoulometric plot implies existence of the diffusional type pattern. Under such conditions, the dependence of Q on $t^{1/2}$ can be effectively described in terms of the integrated Cottrell equation:

$$\left[Q/t^{1/2}\right] = 2nF\pi^{1/2}r^2 \left[D_{\text{app}}^{1/2}C_0\right] \quad (1)$$

Fig. 3 DEIS impedance spectra obtained for the NiHCF film (as for Fig. 2) during **a** oxidation and **b** reduction cycles



propagation, concentration of redox centers, and other parameters either have been discussed above or have their usual significance. From the slope, $[Q/t^{1/2}]$, which is determined from the linear portion of the dependence of Q on $t^{1/2}$, the kinetic parameter, $[D_{\text{app}}^{1/2}C_0]$ can be estimated. The absence of any sizeable negative intercept in the chronocoulometric plot (Fig. 2, inset) permits us to assume that kinetic or ohmic limitations are relatively negligible. Estimation of the apparent diffusion coefficient (D_{app}) has been achieved from the integrated Cottrell equation (Eq. 1) upon assumption of $C_0=0.5 \text{ mol dm}^{-3}$ [23, 28]. Thus, D_{app} values obtained for NiHCF film exposed to $0.5 \text{ mol dm}^{-3} \text{ K}_2\text{SO}_4$ electrolyte have been found in the range from 5×10^{-9} to $6 \times 10^{-9} \text{ cm}^2 \text{ s}^{-1}$, and they are comparable to those reported earlier in KCl electrolyte [28].

To get better insight into the system's ability to propagate charge, the NiHCF films on glassy carbon were further analyzed using recently proposed and developed approach, DEIS [33–35]. In the first step, the perturbation signal (being the sum of selected sine waves of set frequencies, phases shifts, and amplitude) was composed in a manner described earlier [33–35] and, subsequently, provided to the potential input of a potentiostat. Later, a short-time Fourier transform analysis was utilized to obtain the impedance spectra for the electrochemical processes. Figure 3 illustrates the impedance spectra obtained for the NiHCF film (as for Fig. 2) during (a) oxidation and (b) reduction cycles. While the frequency range was from 20 to 16,000 Hz, the sampling frequency was 40,000 samples per second, and the window length covered 4,000 samples. Furthermore, the frequency resolution was 10 Hz, and each spectrum was calculated for a region of the dc voltage change of 3 mV. It is noteworthy that both anodic (Fig. 3a) and cathodic (Fig. 3b) portions of spectra have regular forms [33–35]. In particular, the observed lines are iso-frequency lines that change monotonically with the applied potential. The observed minima (Fig. 3) correspond to the respective oxidation and reduction peaks of Fig. 2. An important issue is that, in the 0.4–0.6 potential range, the charge-transfer resistances of both anodic and cathodic processes drastically diminish and make electron transfers (charge mediation) feasible.

Solid-state electrochemical characterization

Because the intended application of NiHCF is as mediating material in the absence of contact with liquid electrolyte, further diagnostic experiments have been done using the appropriate solid-state methodology. The feasibility of performing solid-state voltammetric measurements of mixed-valent NiHCF pressed pastes under sandwich configuration was established earlier [32]. The mobility of

structural K^+ ions was found to be strongly dependent on the system's degree of hydration. Under typical ambient conditions (80–90% humidity), the systems were sufficiently hydrated (around eight to ten molecules per metal hexacyanoferrate) to assure good mobility of potassium ions. The transport of electrons was explained in terms of electron hopping (self-exchange). In the absence of liquid electrolyte, electron transfers were coupled to the displacement of structural counterions (hydrated K^+) and, thus, electroneutrality was preserved. Furthermore, solid-state voltammetric investigations are possible under two-electrode sandwich configuration because a mixed-valent NiHCF system contains hexacyanoferrate(III,II) redox centers that can be simultaneously oxidized or reduced at interfaces formed by the opposing electrodes [30, 31]. A representative solid-state voltammetric-type response (current versus applied potential differences) of our mixed-valent NiHCF nickel(II) hexacyanoferrate(II,III) material (pasted powder) is shown in Fig. 4. As expected, for two-electrode solid-state voltammetry (sandwich configuration), the response is in a form of voltammetric peaks symmetrical around the point of zero with respect to current and potential. It should be remembered that the cell operates in a manner analogous to classical bipotentiometry in which potential differences are applied to two identical electrodes and scanned linearly with time. It is noteworthy that the voltammetric peak currents of Fig. 4 are proportional to the square root of scan rate up to at least 250 mV s^{-1} (inset of

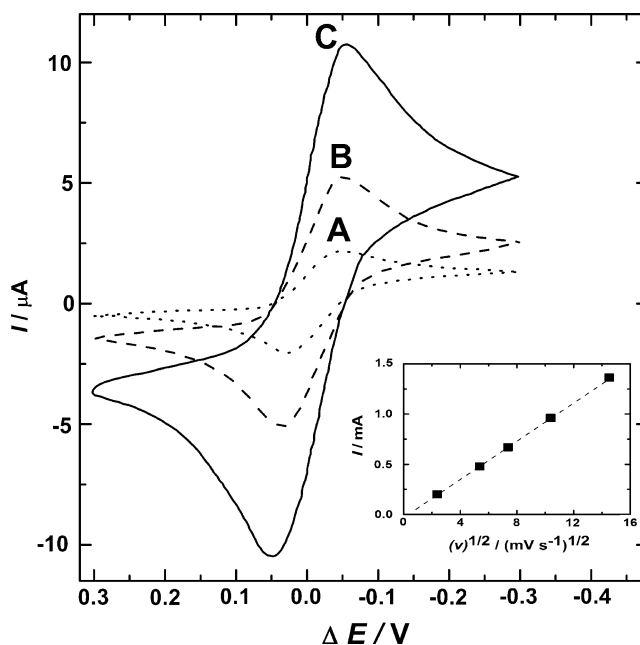


Fig. 4 Solid-state cyclic voltammetric responses for nickel(II) hexacyanoferrate(III,II) [1:1] bulk material (powder) that was pressed between two sandwich-forming electrodes of the design of Fig. 1. Scan rate, 10 mV s^{-1} . Inset illustrates the peak current dependence on scan rate

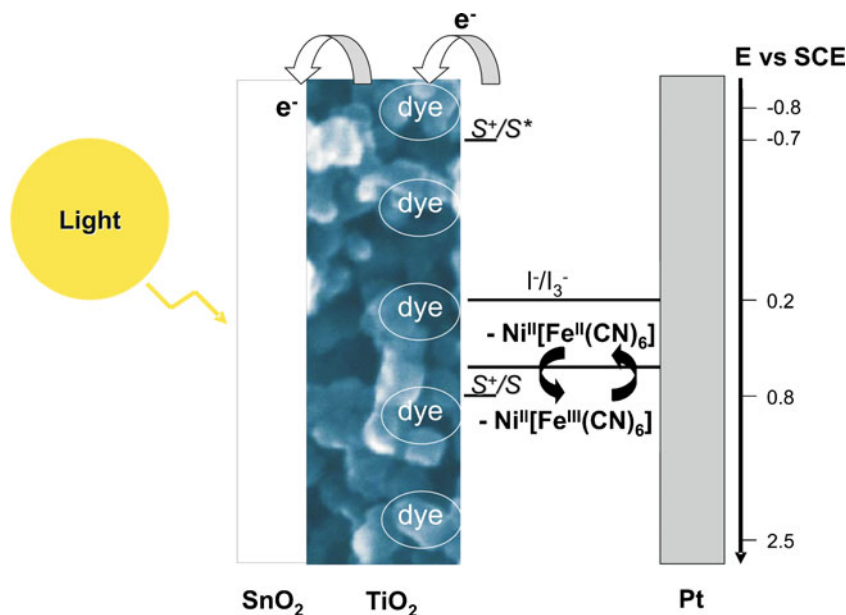
Fig. 4). The result is consistent with the existence of the effectively diffusional charge propagation mechanism predominantly driven by electrochemically generated concentration gradients of mixed-valence hexacyanoferrate(II,III) sites across the sandwiched material. The currents are obviously maximized when the ration of Fe^{II} to Fe^{III} sites is equal 1:1, i.e., under conditions where the concentration of the hexacyanoferrate(III,II) mixed-valent sites is the largest. Completely reduced or oxidized nickel hexacyanoferrate pastes are not electroactive under two-electrode sandwich configuration.

Another important issue is the degree of hydration because K⁺ ions are transported in the hydrated form. It was reported earlier that the K⁺ cation mobility was largely impeded upon dehydration [32]. Although not optimized yet, we have found that the NiHCF material containing roughly 10 to 15 stoichiometric water molecules is a well-behaved system for which the applied potential differences are capable of forcing not only electrons but also mobile-hydrated K⁺ ions to flow in response. In such a solid material as NiHCF, the metal (iron) redox sites are immobilized, the macroscopic diffusion does not operate, and the actual mass transport originates from the simultaneous displacement of electron and mobile counterions. On the whole, we can conclude that, in the absence of the external liquid electrolyte phase, NiHCF pressed pastes can act as mediators in which propagation of charge proceeds effectively according to diffusional mechanism.

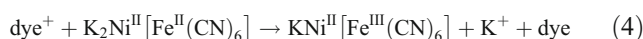
Performance of solar cell with inorganic mediator

Figure 5 illustrates a design of a DSSC utilizing inorganic mediator (NiHCF). The photoanode is made of mesoporous

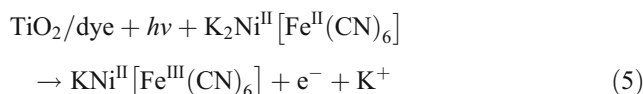
Fig. 5 Design of dye-sensitizer solar cell in which mixed-valent NiHCF pasted powder of Fig. 4 was used as inorganic charge relay (redox mediator). Approximate values of redox potentials of the $-\text{Ni}^{\text{II}}[\text{Fe}^{\text{III,II}}(\text{CN})_6]$ system, the commonly used I^-/I_3^- couple and of the dye (S^+/S) are compared using the calomel electrode scale



dye-sensitizer TiO₂ semiconductors. It receives electron from the photo-excited dye, which is thereby oxidized, and which in turn oxidized the mediator, a redox species dissolved in electrolyte. The mediator (the oxidized form of nickel(II) hexacyanoferrate(III)) is regenerated by reduction at the cathode by the electrons circulated through the external circuit. Cathode is in a form a platinized conducting glass electrode. Excited dye is in the cationic form while it is transferring e⁻ to the TiO₂ conducting band. The dye (Fig. 6) is capable of oxidizing the reduced form, nickel (II) hexacyanoferrate(II). The sequence of reactions in our dye-sensitizer solar cell is as follows:



The overall reaction occurring at the photoanode may be represented simply as:



Although the formal potential of our system—nickel hexacyanoferrate (approximately 0.6 V vs. SCE) is still more negative than that (approximately 0.85 V vs. SCE) of the ground state of N3 dye [cis-dithiocyanatobis (4,4'-dicarboxylic acid-2,2'-bipyridine) ruthenium(II)], an important issue is that the potential is more positive relative to the

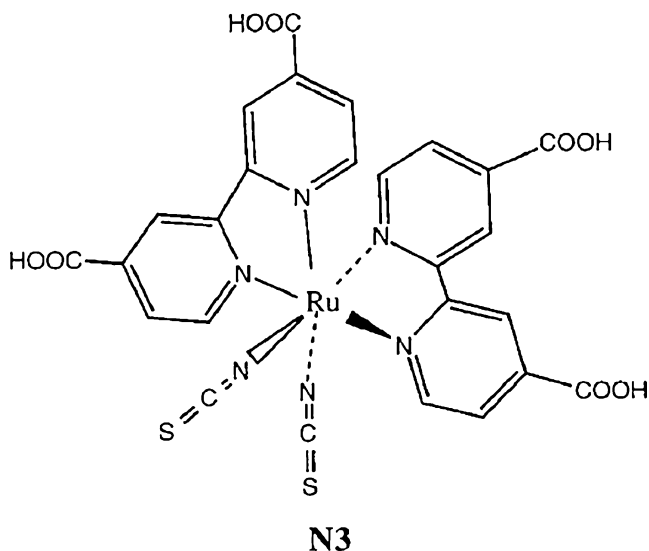


Fig. 6 Molecular structure of the N3 dye

iodide/triiodide couple (0.15 V vs. SCE). In principle, the latter phenomenon should result in larger photopotentials produced by the photocell.

Figure 7 shows the photocurrent action spectrum of a typical cell under short-circuit conditions. The given values are not corrected for reflection and absorption losses. The spectrum closely matches the absorption spectrum of the dye [1, 8] thus confirming that the observed photocurrent arises from electron injection by the sensitizer. The maximum value of photocurrent occurs at 560 nm.

Figure 8 illustrates dependence of the density of generated photocurrent on potential. Under the one-sun illumination of the cell, a short-circuit photocurrent density of 8 mA/cm² is produced. Along with the voltage of 790 mV and fill factor of 0.7, the result implies the energy efficiency exceeding 4% (at one sun).

The data of Fig. 9 are consistent with the reproducible behavior during multiple photoelectrochemical experi-

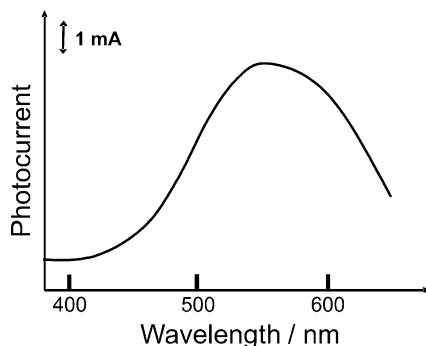


Fig. 7 Action spectrum of the dye-sensitized solar cell (DSSC) utilizing NiHCF charge relay. Light intensity, 1.5 full sunlight (100 mW/cm²)

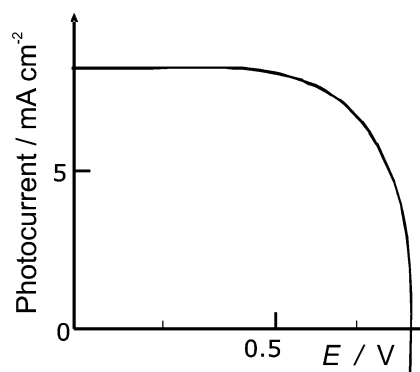


Fig. 8 Photocurrent density–voltage characteristics of DSSC utilizing NiHCF charge relay. Light intensity, 1.5 full sunlight (100 mW/cm²)

ments. Several cells have been examined, and all of them here produced comparable short-circuit current densities (within ±20%). During repetitive long-time measurements, almost identical photocurrents are obtained. After 3 days of intense utilization, the system has been still stable, and the photocurrent produced was reproducible within ±20%.

Conclusions

On the basis of our measurements with nickel(II) hexacyanoferrate(II,III), i.e., the polynuclear inorganic mediator, it can be concluded that such a mixed-valent cyanometallate system (pasted powder) is capable of fairly fast charge propagation involving electron transfers accompanied by structural potassium counterion displacements [23, 32, 38]. Such inorganic structures can form conducting interface with the nanostructured dye-modified semiconductor. The mixed-valent metal hexacyanoferrate can act as solid inorganic charge redox mediator characterized by fairly positive potential. Although morphology of the redox mediator has not been optimized yet, pasted powders of nickel(II) hexacyanoferrate(II,III) could be of utility as a charge relay in a dye-sensitized solar cell.

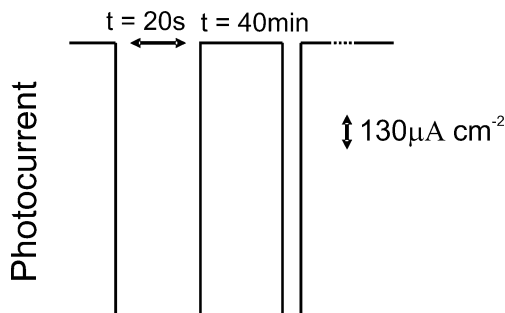


Fig. 9 Multiple illumination pulses on the NiHCF-containing DSSC. Light intensity, 1.5 full sunlight (100 mW/cm²)

Acknowledgments This work was supported by Ministry of Science and Higher Education (Poland) under grant no. N204 031235.

Open Access This article is distributed under the terms of the Creative Commons Attribution Noncommercial License which permits any noncommercial use, distribution, and reproduction in any medium, provided the original author(s) and source are credited.

References

1. O'Regan B, Graetzel M (1991) *Nature* 353:737
2. Benkstein KD, Kopidakis N, van de Lagemaat J, Frank AJ (2003) *J Phys Chem B* 107:7759
3. Benkoe G, Skarman B, Wallenberg R, Hagfeldt A, Sundstroem V, Yartsev AP (2003) *J Phys Chem B* 107:1370
4. Nakade S, Saito Y, Kubo W, Kitamura T, Wada Y, Yanagida S (2003) *J Phys Chem B* 107:8607
5. Nazeeruddin MK, Pechy P, Renouard T, Zakeeruddin SM, Humphry-Baker R, Liska P, Cevey L, Costa E, Shklover V, Spiccia L, Deacon GB, Bignozzi CA, Graetzel M (2001) *J Am Chem Soc* 123:1613
6. Thomas KRJ, Lin JT, Hsu YC, Ho KC (2005) *Chem Commun* 4098
7. Velusamy M, Thomas KRJ, Lin JT, Hsu YC, Ho KC (2005) *Org Lett* 7:1899
8. O'Regan B, Moser J, Anderson M, Graetzel M (1990) *J Phys Chem* 9:8720
9. Nazeeruddin MK, Kay A, Rodicio I, Humphrey-Baker R, Mueller E, Liska P, Vlachopoulos N, Graetzel M (1993) *J Am Chem Soc* 115:6382
10. Cahen D, Hodes G, Graetzel M, Guillemoles JF, Riess I (2000) *J Phys Chem B* 104:2053
11. Chen X, Mao SS (2007) *Chem Rev* 107:2891
12. Wang P, Zakeeruddin SM, Moser JE, Humphry-Baker R, Graetzel M (2004) *J Am Chem Soc* 126:7164
13. Nusbaumer H, Zakeeruddin SM, Moser JE, Graetzel M (2003) *Chem Eur J* 9:3756
14. Nusbaumer H, Moser JE, Zakeeruddin SM, Nazeeruddin MK, Graetzel M (2001) *J Phys Chem B* 105:10461
15. Sapp SA, Elliot M, Contado C, Caramori S, Bignozzi CA (2002) *J Am Chem Soc* 124:11215
16. O'Regan B, Lenzmann F, Muis R, Wienke J (2002) *Chem Mater* 14:5023
17. Kumara GRA, Kaneko S, Okuya M, Tennakone K (2002) *Langmuir* 18:10493
18. Nogueira AF, Durrant JR, DePaoli MA (2001) *Adv Mater* 13:826
19. Stergiopoulos T, Arabatzis IM, Katsaros G, Falaras P (2002) *Nano Lett* 2:1259
20. Bach U, Lupo D, Comte P, Moser JE, Weissortel F, Salbeck J, Spreitzer H, Graetzel M (1998) *Nature* 395:583
21. Wasserscheid P, Welton T (2002) *Ionic liquids in synthesis*. Wiley-VCH, Weinheim
22. Lin C, Bocarsly AB (1991) *J Electroanal Chem* 300:325
23. Malik MA, Miecznikowski K, Kulesza PJ (2000) *Electrochim Acta* 45:3777
24. Joseph J, Gomathi H, Prabhakara Rao G (1991) *Electrochim Acta* 36:1537
25. Kubota LT, Gushikem Y (1993) *J Electroanal Chem* 362:219
26. Bacskai J, Martinusz K, Czizrok E, Inzelt G, Kulesza PJ, Malik MA (1995) *J Electroanal Chem* 385:241
27. Kulesza PJ, Malik MA, Schmidt R, Smolinska A, Miecznikowski K, Zamponi S, Czerwinski A, Berrettoni M, Marassi R (2000) *J Electroanal Chem* 487:57
28. Malik MA, Kulesza PJ, Marassi R, Nobili F, Miecznikowski K, Zamponi S (2004) *Electrochim Acta* 49:4253
29. Zamponi S, Berrettoni M, Kulesza PJ, Miecznikowski K, Malik MA, Makowski O, Marassi R (2003) *Electrochim Acta* 48:4261
30. Kulesza PJ, Malik MA (1999) In: Wieckowski A (ed) *Interfacial electrochemistry—theory, experiment and applications, solid-state voltammetry* 673. Marcel Dekker, New York
31. Kulesza PJ, Cox JA (1998) *Electroanalysis* 10:73
32. Kulesza PJ, Galus Z (1992) *J Electroanal Chem* 323:261
33. Darowicki K (2000) *J Electroanal Chem* 486:101
34. Darowicki K, Slepski P (2003) *J Electroanal Chem* 547:1
35. Darowicki K, Kawula J (2004) *Electrochim Acta* 49:4829
36. O'Regan B, Schwartz DT (1996) *J Appl Phys* 80:4749
37. Lindstrom H, Magnusson E, Holmberg A, Sodergren S, Lindquist SE, Hagfeldt A (2002) *Solar Energy Mater Solar Cells* 73:91
38. Kulesza PJ, Dickinson VE, Williams ME, Hendrickson S, Malik MA, Miecznikowski K, Murray RW (2001) *J Phys Chem B* 105:5833